2010

Experimental Investigation of Frost Growth on Microchannel Heat Exchangers

Ehsan Moallem
Oklahoma State University

Lorenzo Cremaschi
Oklahoma State University

Daniel E. Fisher
Oklahoma State University

Experimental Investigation of Frost Growth on Microchannel Heat Exchangers

Ehsan Moallem[1]*, Lorenzo Cremaschi[1], and Daniel E. Fisher[1]

[1]* School of Mechanical & Aerospace Engineering, Oklahoma State University, Stillwater, OK, 74078, USA (moallem@okstate.edu)

ABSTRACT

In this paper, new measurements of frost nucleation time and growth rate on a small 0.3m by 0.3m microchannel heat exchanger are presented. During the data reduction, fin surface temperature, uniform air temperature distribution, air lift and drag effects, and air velocity distribution were carefully evaluated and taken into consideration. The microchannel fin surface temperature, entering air face velocity, relative humidity and the amount of water retained within the fins were varied in a parametric fashion in order to identify the predominant factors affecting the frosting performance. Results show that the water retention and air face velocity do not have a significant impact on the frosting cycle while surface temperature and air relative humidity affect the frosting time considerably. Digital videos of frost formation confirmed that frost does not nucleate from large water droplets within the fins but mainly from the leading edges at the front of the fins.

1. INTRODUCTION

Heat pump systems are used for cooling and heating of buildings all year round. Microchannel-type heat exchangers have recently been adopted by the heat pump industry because of their compactness and efficiency in residential and commercial applications. However, their usage as outdoor evaporators results in faster frost growth and frequent defrost cycles, which ultimately limits the seasonal heating performance during winters. Previous studies showed that heat pumps with microchannel type outdoor evaporators defrost more often than fin-and-tube heat pump units, operating under similar conditions, and the overall heating seasonal performance factor is in most cases are lower than conventional fin-and-tube heat exchangers (Kim and Groll, 2003; Padhmanabhan et al., 2008). A better understanding of frost formation on microchannel heat exchangers is necessary to identify the root causes of this problem.

The fundamental understanding of the heat and mass transfer characteristics of coils during frosting and defrosting transient periods are still not well-known. Especially most of the previous results are based on a limited range of experimental tests on different simple geometries like bank of flat fins or on more realistic geometries such as fin and tube and flat tube heat exchangers. For these cases, the effects due to fin geometry and water retention are difficult to isolate and quantify because several parameters have been varied at once (Na and Webb, 2004; Xia et al., 2005; Xia et al., 2006; Yang et al., 2006). Other fundamental studies focused on simplified geometries, such as flat plates or channel flows between parallel flat plates (Lenic et al., 2009; Lüer and Beer, 2000). The complexity of the phenomena makes the theoretical analysis problematic and increases the difficulty in accurately measuring the influence of fin surface temperature, fin geometry, and fin surface energy on frost growth (Ohkubo, 2006; Shin et al., 2003). Measuring frost weight on an entire coil mounted on a heat pump system is not only experimentally difficult, but most of the time impractical and inaccurate. Consequently, work in the literature was also conducted on frost growth on small scale microchannel heat exchangers installed in experimental facility design ad-hoc to reproduce the operating conditions (Verma et al., 2002; Xia et al., 2005). While this approach allows the direct measurement of the frost weight, caution must be taken during the data reduction and the extension of the experimental outcomes to actual coils.

In this paper, we present new measurements of frost growth rate and defrost performance on a microchannel heat exchanger using Ethylene Glycol 50/50 solution for simulating the refrigerant side and with the coil operating at the typical environmental conditions as the ones of outdoor coils of heat pump systems during winter periods. All the conditions controlled within the AHRI 210/240 specified tolerances. Non-uniform air temperature distribution, air

lift and drag effects, and air velocity distribution were taken into considerations during the data reduction. Some tests were repeated several times until criteria for air even temperature and velocity distribution were satisfied. A precision scale was employed to record frost weight during tests and the experimental procedure showed improved accuracy with respect to frost estimates from heat balance and humidity difference methods. Frost-defrost cycles were performed on a microchannel coil. The microchannel surface temperature, coil face entering air velocity, air relative humidity and water retention were varied in a parametric fashion to identify the predominant factors affecting the frosting performance. Frost thickness was experimentally measured using a digital CCD video scope camera at and pressure drop, frost weight, and frosting time were also recorded simultaneously. This method was successfully employed before and provided very accurate measurements of the frost growth rate (Moallem et al., 2010; Xia and Jacobi, 2005).

2. EXPERIMENTAL SETUP

2.1 Heat Exchanger Specifications

The microchannel heat exchanger used in the experiments is shown in Figure 1 and it consists of a small 0.305m×0.305m 1 row aluminium louvered fin microchannel heat exchanger with 27 vertical tubes and 25.4mm depth. There are 4 rectangular shaped ports in each tube with dimensions of 5mm by 1mm. Folded fins are 1.25mm apart and have a 0.1mm thickness.

2.2 General System Setup

The test coil was set inside a controlled low temperature wind tunnel facility, which is schematically shown in Figure 1. The low temperature wind tunnel consisted of a closed loop duct system containing a centrifugal fan, a large refrigeration coil, an electrical heater, turning vanes, nozzles for flow measurements, humidifiers, thermocouples, pressure reading tubes, dew point meters and a digital scale. Air enters the test coil at 1.7°C dry bulb and 0.6°C wet bulb temperatures (35/33°F db/wb) unless otherwise specified. This yields an entering relative humidity of about 82% during the experiments. The approaching air velocity is controlled by a variable speed fan and ranged from 0.7 to 1.5 m/s. These inlet conditions were controlled within a precision specified in the standard AHRI 210 for heat pump system performance rating. Three ultrasonic humidifiers were installed at the top section inside the wind tunnel to guarantee sufficient time for mixing and to achieve the desired humidity in the air stream. The cooling load of the tunnel was met by a large refrigeration coil connected to a low temperature chiller. Air leaving the refrigeration coil was heated by a 1.4 kW variable power electrical heater, whose capacity was adjusted to accurately set the air temperature approaching the microchannel coil.

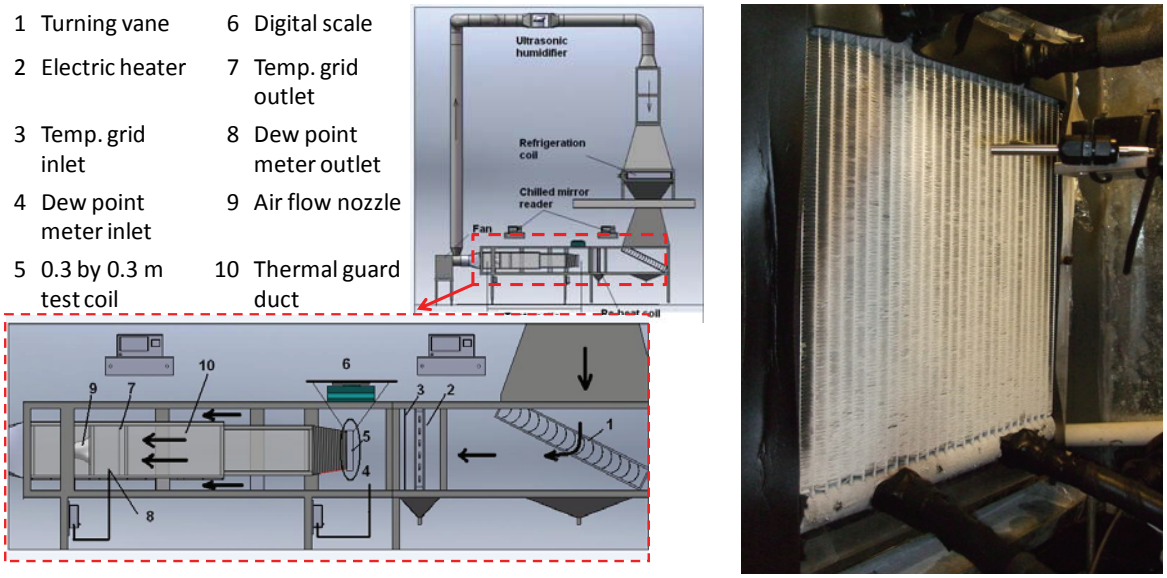

Figure 1: Schematic of the air wind tunnel for low temperature frosting experiments (left) and Image of the microchannel coil under frosting inside the low temperature air wind tunnel (right).

Extra care was taken to improve the heat balance and minimize the effect of parasitic heat gains from the surroundings to the test coil. A dual concentric square duct tunnel was designed for this purpose, and it is shown in the bottom schematic of Figure 1. The flow nozzle and temperature sensors were mounted inside the inner tunnel. Sixteen calibrated T-Type copper constantan thermocouples (4×4 grid) were used to calculate the average air temperature and the air temperature uniformity at the front section and after the test coil. The air pressure drop across the coil was measured by a pressure difference transducer and air humidity was measured using two chilled mirror dew point meters before and after the coil test section. A secondary refrigeration loop was built to accurately set the conditions to the microchannel coil, which is the test coil component 5 in Figure 1. The secondary loop consisted of cold and hot storage tanks, a Coriolis flow meter, two high precision platinum RTDs and a variable speed gear pump. It circulated a solution of water and Ethylene Glycol 50/50 volume and it controlled the inlet refrigerant temperature to the test coil in the range from -26 to 0°C during the frosting tests and with a constant flow rate of 0.345 kg/s. The temperature of entering refrigerant to the coil was controlled within ±0.25°C and it was chosen as the main variable that characterizes the fin surface temperature. During each test it was stable and kept constant. Fine gauge thermocouples were attached to the fins but the contact resistance was quite high and the readings from thermocouples represented an average temperature between fin and local air film surrounding the surface. As soon as the tips of the thermocouples were covered by the frost, the temperature readings were closer to the fin temperature.

The uncertainty in total heat transfer rate was calculated to be within ±10% for the refrigerant side and around ±9% for air side. The heat balance error was well within 5% during dry heat transfer tests and increased to 10% for the initial periods of the wet and frost tests. Because of the transient nature of the experiments, the heat balance error increased to up to 20% in average and occasionally reached 30% at the end of the frost period. The authors believed that this deviation is due to transient heat conduction effects, thermal mass storage effects, and frost densification effects. Furthermore, the chilled mirror dew point meters provided inherently uncertain measurements when near to frosting conditions and they might lag the actual reading of the water vapour removal from the air stream. Even thought the digital scale had an nominal accuracy of ±0.2 g, the authors concluded that frost weights uncertainty was about ±5g.. This values might seems rather pessimistic but it was obtained from a detailed analysis of the set up, by checking the residual stresses in the pipe connections, by taking into account hysteresis of the instrumentation, friction, and air lift and drag effects. Ultimately an extensive calibration of the facility was conducted before commencing the experiments. More details of the test facility, instrument accuracies, control tolerances, calibration and uncertainty analysis are provided by Cai (2009) and Moallem et al. (2010).

2.3 Frost Weight Measurement

The microchannel test coil was suspended in the wind tunnel and hung from the digital scale (comp. 6 in Figure 1), which recorded the frost growth rate during the tests. A very thin plastic film was installed loosely before and after the test coil to provide an air seal between the inner duct and the tunnel. Two flexible polymer hoses were used for the refrigerant connections; they were clamped between the secondary loop and the test coil refrigerant ports. Each flexible hose was about 1 meter long, and it was coiled one time around itself before it was connected to the port of the heat exchanger. This configuration eliminated any structural constraints to the vertical displacements of the test coil when frost accumulated on its surface.

In this study, the primary measurement to obtain the frost mass accumulated on the fins was the weight increase of the whole coil during the test. Through a series of calibration tests, it was observed that the effects of air lift and drag on the test coil caused a systematic error in the measurements of the frost weight. To eliminate this error, the fan was periodically stopped 4 to 5 times for short intervals during each frosting experiment. Each pause was no longer than one minute and allowed the air in the tunnel to come to a rest. In the absence of forced air flow, the test coil was temporarily released from the effects of lift, drag, and static friction, and a new equilibrium position was achieved. Once the frost weight was sampled and recorded, the fan was started again and the test continued until the next pause. It should be noticed that only the air flow in the tunnel was interrupted while the refrigerant flow was run constantly during the entire experiment. An investigation was performed to verify that the test procedure did not interfere with the actual frost growth process in the heat exchanger. The reader can find the details in the work by Moallem et al. (2010).

2.4 Frost Thickness Measurement

A typical frost pattern of frost growth on the microchannel coil is shown in Figure 3. The frost thickness was captured by a high resolution short focus CCD (Charge-Coupled Device) camera, which included a 1 meter extended mini probe head. The probe tip of the CCD camera was installed at the front of the test coil and mounted on a programmable robotic arm connected to three stepper motors. The images were processed after each

experiment to obtain the frost thickness in each location. The accuracy of the frost thickness measurements was about 0.03mm. Further details of the programmable robotic arms, camera controls and thickness measurement details are provided by Carroll and Peterson (2009) and Moallem et al. (2010).

3. RESULTS AND DISCUSSION

To evaluate the influence of each factor on frost formation on the coil, a series of experiments were conducted at various air and refrigerant conditions. All tests were conducted with the heat exchangers initially in dry surface conditions and at constant air temperature and constant refrigerant flow rate except when specified. For the air side, the fan had a constant RPM throughout the test. The coil face air velocity was set at the beginning of the test and then it dropped as the frost formed on the coil. The test was terminated when the face velocity reached 75% of its initial value. This method was preferred with respect to constant velocity tests since it is closer to the actual application. Air volumetric flow rate was measured using a flow nozzle section and air face velocity was calculated from the frontal area of the microchannel coil. The effect of surface temperature and water retention are shown in Figure 2. The entering refrigerant temperature (ERT) is the controlled variable and it is kept constant during each test. The surface temperature is an average temperature of the fins and was estimated from theoretical and numerical analysis (Padhmanabhan et al., 2010). The surface temperatures are for initial dry conditions and they decreased as frost growth on the coil. Three dry-start tests at different ERT temperatures of -6.7ºC, -9.4ºC and -12.2ºC were compared first. Lower ERT resulted in lower fin surface temperature and the frost growth rate decreased when the fin temperature increases from -6 to -3°C and the frosting cycle time almost doubled. If the fin temperature is lowered to about -9°C the frosting time resulted only about 15 minutes. Two additional tests were performed to study the effect of water retention for similar fin temperature. The baseline test for this comparison is the test at ETR of -9.4ºC dry start, with an estimated initial fin temperature of -6°C. In dry start conditions, the surface was initially dry at the beginning of the test. To achieve dry start conditions the coil was exposed to room ambient temperature overnight. Then it was brought to 35/33°F db/wb temperature inside the wind tunnel in 4 to 5 hours and finally the refrigerant was pumped through the coil only right before starting the test. At fin temperature of -6ºC and dry start conditions the frosting time was about 27 minutes and the frost mass was about 135g. Next, the ERT was fixed at -9.4ºC and water was artificially sprayed on the front area of the coil. Visible droplets were observed in between the fins at the beginning of the test. 200g and 500g of water were retained in the coil before starting the frosting cycle. These conditions replicate similar scenarios of when the coil is partially wet or fully wet after multiple defrost cycles.

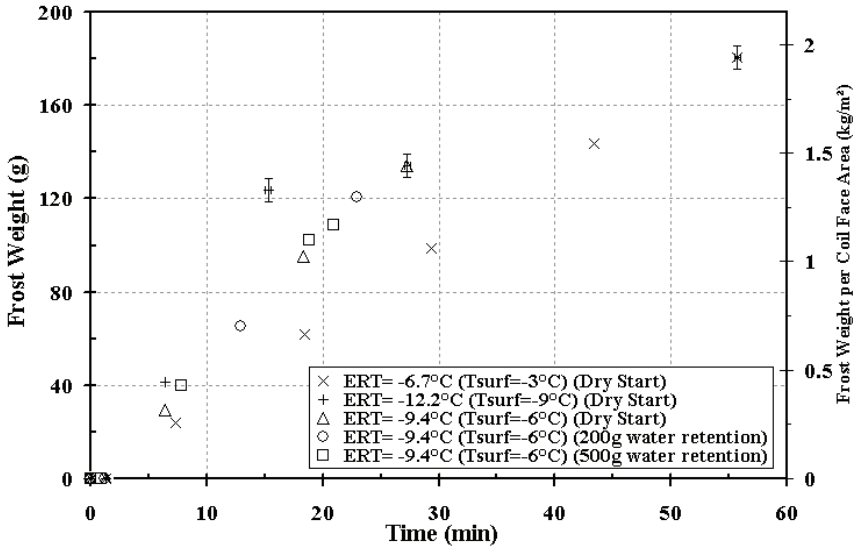

Figure 2: Effect of surface temperature and water retention on microchannel coil frost weight under constant air temperature (1.7ºC/0.6ºC db/wb AHRI), air velocity starting from 1.0m/s at the beginning dropping to 0.75m/s at the end of the test and constant refrigerant (ethylene glycol) flow rate (0.345kg/s).

As soon as the refrigerant was pumped into the microchannel coil, the water droplets froze up in between the fins. The scale was set to zero at the very beginning of each test in order to measure only the weight of the frost nucleated from the water vapor in the air stream. The weight of the ice beads in between the fins is not included in the Figure 2. We can observe that the water droplets do not affect the rate of frost growth and for a large amount of water retained in the coil, the frosting time decreases by only 6 minutes. This seems to suggest that surface temperature has a direct and significant effect on the weight of frost growth while water retention has minor or negligible effect on it.

Image recordings of the coil during the tests were performed and an example is shown in Figure 3. From the images and videos it seems that frost does not nucleate from the water droplets that turned into ice beads and bridged the fins but frost always started from the microchannel tube wall and fin leading edges.

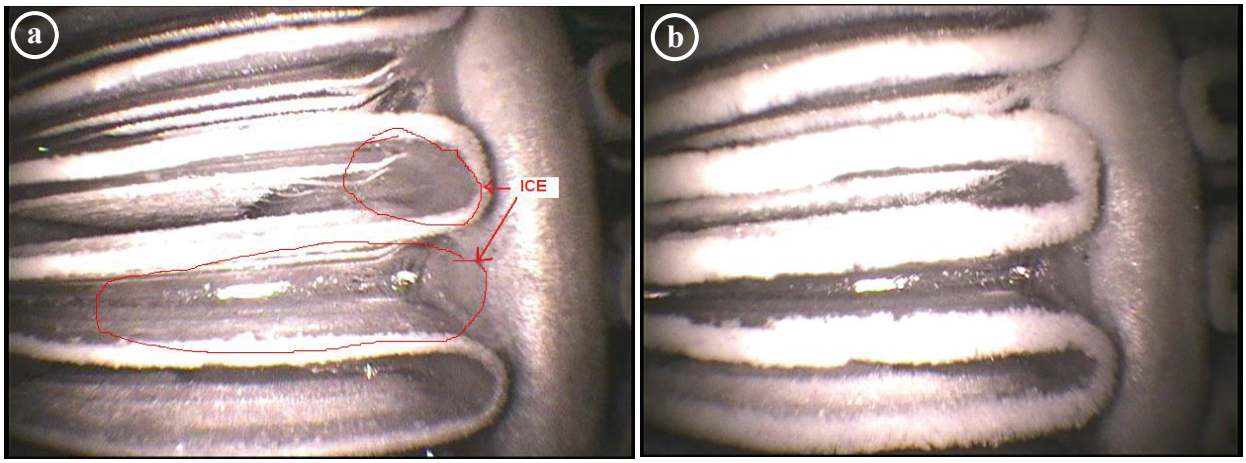

Figure 3: Frost formation on a microchannel coil after a defrost cycle a) Right after starting a frost cycle b) near the end of the same frost cycle. Pictures are taken from frozen droplets of water remained between fins from previous defrost cycles (shown by red line tagged as ice). Pictures show that frost does not nucleate or start from droplets of water from previous cycles, but starts from fin edges which are the coldest spots.

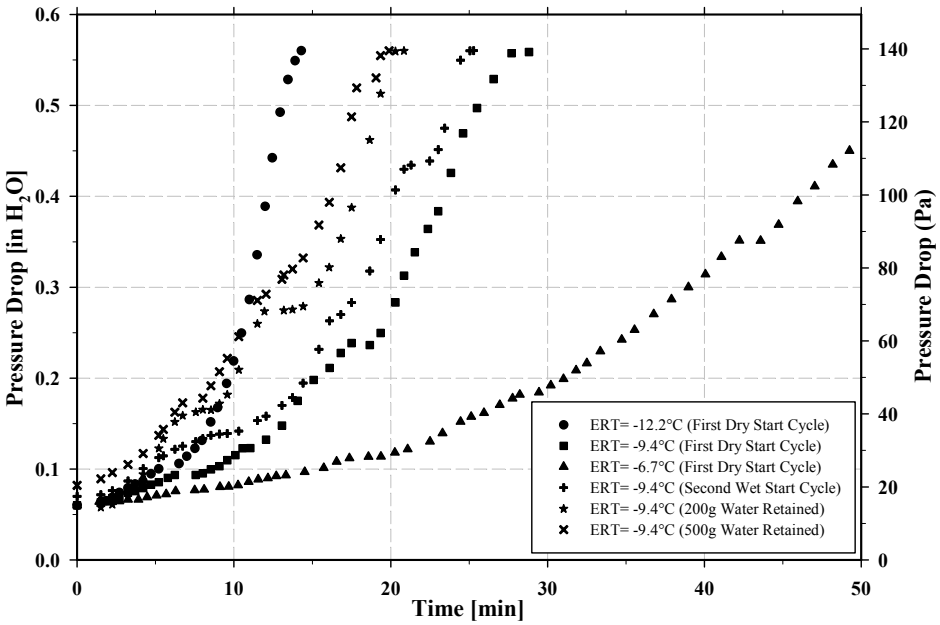

Figure 4: Effect of surface temperature and water retention on microchannel coil air side pressure drop under constant air temperature (1.7ºC/0.6ºC db/wb AHRI) and velocity starting from 1.0m/s at the beginning dropping to 0.75m/s at the end of the test, constant refrigerant flow rate (0.345kg/s).

Pointing the CCD camera directly on few water droplets trapped between the fins, as shown in Figure 3a, revealed that as soon as the frost cycle starts, water droplets freeze up in their locations. As shown in Figure 3b, the frost does not deposit on the frozen droplets but still nucleates from the fin edges and tube walls. These locations are the coldest spots of the coil and local stagnation areas for the air stream, for which considerable heat and mass transfer processes seems to occur. These ice beads partially blocks the air flow and increase the air pressure drop through microchannel coil. However, these effects are not significant even with a large amount of water droplets dispersed on the fins. Similar results are observed in Figure 4.

The effects of surface temperature and coil water retention on air side pressure drop across the microchannel coil are shown in Figure 4. Lower surface temperature results in higher air side pressure drop. From Figure 2 and Figure 4 we observe that water retention has small effect on frost weight growth rate on the coil but it has a more distinct effect on the air pressure drop. With 200g or 500g of water retained in the coil, the amount of water that fills up the space in between the fins, reduced the frosting time from 27 minutes in dry conditions to 23 and 21 minutes respectively.

The effect of entering air relative humidity is shown in Figure 5. As it was expected, higher air relative humidity caused faster frost growth rate and if relative humidty increased from 82 to 92%, the frosting time decreased from 27 to 16 minutes, respectively. More water vapor in the air stream increased the absolute humidity, which augmented the partial pressure of the vapor in the air stream. The pressure difference between the water vapor in the air stream and the water vapor at the frost interface is the driving force for the mass transfer process. Thus, high relative humidities result in larger pressure gradients and faster frost growth on the fins.

Another parameter that was investigated was the coil face air velocity and its effect on frost formation is shown in Figure 6. All the tests started with initial velocity of 1.4, 1.0 and 0.75 m/s respectively and they were terminated when the air velocity reached 75% of their initial values. The fan rotational speed was kept constant during each test so the volumetric flow rate of flow dropped continuously during the test. As it is shown in the Figure 6, tests have the same frost time approximately that is 25, 27 and 28 minutes. Frost weight growth rate are very similar in 1.0m/s and 0.75m/s tests and it seems that air velocity has negligible effect on the frost formation. The weight of frost for the 1.4m/s test is higher but the frosting time is still similar to the other cases. The authors speculate that the higher velocities affect the distribution of the frost along the depth of the fin. Thus, even thought more mass is accumulated on the fin, the rate at which the free flow area is blocked did not change.

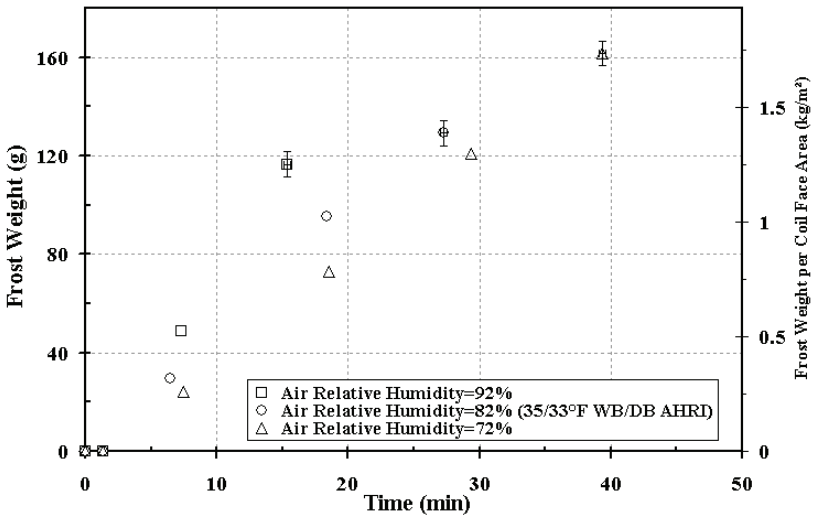

Figure 5: Effect of entering air relative humidity on frost accumulation weight on microchannel under constant air temperature (1.7ºC) and velocity starting from 1.0m/s at the beginning dropping to 0.75m/s at the end of the test, constant entering refrigerant temperature (-9.4ºC) and flow rate (0.345kg/s).

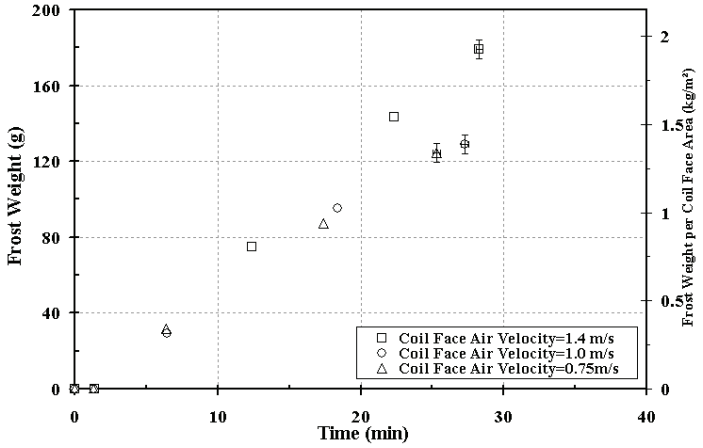

Figure 6: Effect of coil face air velocity on microchannel coil frost weight under constant air temperature (1.7ºC/0.6ºC db/wb AHRI) and constant refrigerant temperature (-9.4ºC) and flow rate (0.345kg/s).

3. CONCLUSIONS

This study experimentally investigates frost growth on microchannel heat exchangers. Surface temperature and air relative humidity are main factors that affect the frost formation rate and frost time significantly while water retention and air velocity can be accounted as secondary effects that cause minor changes in frost time or frost weight. The experimental results showed that reducing the water droplets retained within the fins, at the end of the defrost cycle, did not have a significant impact on the next frosting cycle time. Digital images of frost growth confirmed that frost does not nucleate from the water droplets trapped within the fins but mainly from the leading edges of the front fins and the tube front edges. These locations are the coldest spots of the coil and local stagnation areas for the air stream, for which considerable heat and mass transfer processes seems to occur. At similar surface temperature, the frosting time was about the same for three different amount of water retained in the microchannel coil, that is, dry coil, partially wet coil, and fully wet coil with large amount of water droplets in it. This seems to indicate that the predominant factors on frost growth are the surface temperature, air relative humidity and the leading edge geometry of the fins. Further studies on frost nucleation sites at front leading edges of the coil, frost distribution along the fins, and methods to extend the air flow blockage should be considered more in details in the future to achieve a better frosting performance for microchannel heat exchangers.

REFERENCES

AHRI, AHRI Standard 210/240-2008, Performance Rating of Unitary Air Conditioning and Air-Source Heat Pump Equipment, AHRI, Ed. 2008.

Cai S. (2009) Design of an Experimental Facility for Measurement of Frost Growth on Heat Exchangers. Master Thesis Mechanical and Aerospace Engineering Department, Oklahoma State University, OK, USA.

Carroll C., Peterson J. (2009) Design and Construction of a Three-Axis Traverse System for an Image Capture in Frost Experiments. Senior Design Report Mechanical and Aerospace Engineering Department, Oklahoma State University, OK, USA.

Kim J.-H., Groll E.A. (2003) Microchannel Heat Exchanger Defrost Performance and Reliability. ASHRAE final report 1195-RP, Atlanta, GA, USA.

Lenic K., Trp A., Frankovic B. (2009) Transient two-dimensional model of frost formation on a fin-and-tube heat exchanger. International Journal of Heat and Mass Transfer 52:22-32.

Lüer A., Beer H. (2000) Frost deposition in a parallel plate channel under laminar flow conditions. International Journal of Thermal Sciences vol. 39:85-95.

Moallem E., Padhmanabhan S., Cremaschi L., Fisher D.E. (2010) Experimental Study of Onset and Growth of Frost on Outdoor Coils of Air-Source Heat Pump Systems. Proceedings of ASME-ATI-UIT, Conference on Thermal and Environmental Issues in Energy Systems May 2010, Sorrento, Italy (in Press).

Na B., Webb R.L. (2004) Mass transfer on and within a frost layer. International Journal of Heat and Mass Transfer 47:899-911.

Ohkubo H. (2006) Advance of 'Study on Frosting Phenomena'. Refrigeration 81:255-9.
Padhmanabhan S., Fisher D.E., Cremaschi L. (2010) A Scaling Approach for Predicting Frost Growth in a Heat Exchanger – Application to Fin-Tube Coil. ASME-ATI-UIT 2010 Conference on Thermal and Environmental Issues in Energy Systems 16 – 19 May, 2010, Sorrento, Italy.
Padhmanabhan S., Fisher D.E., Cremaschi L., Knight J. (2008) Comparison of Frost and Defrost Performance between Microchannel Coil and Fin-and-Tube Coil for Heat Pump Systems. 12th International Refrigeration and Air Conditioning Conference at Purdue West Lafayette, IN, USA, paper no. R2202.
Shin J., Tikhonov A.V., Kim C. (2003) Experimental Study on Frost Structure on Surfaces With Different Hydrophilicity: Density and Thermal Conductivity. ASME Journal of Heat Transfer 125:84-94.
Verma P., Carlson D.M., Wu Y., Hrnjak P.S., Bullard C.W. (2002) Experimentally Validated Model for Frosting of Plain-Fin-Round-Tube Heat Exchangers. Air-Conditioning & Refrigeration Center.
Xia Y., Jacobi A.M. (2005) Air-side data interpretation and performance analysis for heat exchangers with simultaneous heat and mass transfer: Wet and frosted surfaces. International Journal of Heat and Mass Transfer 48:5089-5102.
Xia Y., Hrnjak P.S., Jacobi A.M. (2005) Air-Side Thermal-Hydraulic Performance of Louvered-Fin, Flat-Tube Heat Exchangers with Sequential Frost-Growth Cycles. ASHRAE Transactions, Winter Meeting, Orlando, FL, USA 111:487-495.
Xia Y., Zhong Y., Hrnjak P.S., Jacobi A.M. (2006) Frost, defrost, and refrost and its impact on the air-side thermal-hydraulic performance of louvered-fin, flat-tube heat exchangers. International Journal of Refrigeration 29:1066-1079.
Yang D.-K., Lee K.-S., Song S. (2006) Modeling for predicting frosting behavior of a fin-tube heat exchanger. International Journal of Heat and Mass Transfer 49:1472-1479.

ACKNOWLEDGEMENT

Authors would like to acknowledge the support from Oklahoma Centre for Advancement in Science & Technology (OCAST) and the Building Efficiency Group of Johnson Controls Inc.